Geophysical Research Letters®

Key Points:

- Antarctic Slope Current (ASC) changes under projected, time-varying climate forcings are dominated by meltwater perturbations
- ASC strength undergoes a dramatic, non-linear increase over time, even under linearly-increasing meltwater perturbation
- The non-linear ASC strengthening is due to meltwater accumulation on the shelf and poleward-shifted warm water at depth

Correspondence to:

E. Q. Y. Ong,
ellie.ong@unsw.edu.au;
ellie.ong@monash.edu

Author Contributions:

Conceptualization: Ellie Q. Y. Ong, Matthew H. England
Formal analysis: Ellie Q. Y. Ong
Methodology: Ellie Q. Y. Ong, Matthew H. England
Supervision: Matthew H. England, Edward Doddridge, Navid C. Constantinou
Validation: Ellie Q. Y. Ong, Matthew H. England, Edward Doddridge, Navid C. Constantinou
Writing – original draft: Ellie Q. Y. Ong
Writing – review & editing: Matthew H. England, Edward Doddridge, Navid C. Constantinou

Transient Antarctic Slope Current Response to Climate Change Including Meltwater

Ellie Q. Y. Ong[1,2] , Matthew H. England[2,3] , Edward Doddridge[4] , and Navid C. Constantinou[5,6]

[1]ARC Centre of Excellence for Weather of the 21st Century, Monash University, Clayton, VIC, Australia, [2]Climate Change Research Centre and Australian Centre for Excellence in Antarctic Science, University of New South Wales, Sydney, NSW, Australia, [3]Centre of Marine Science and Innovation, University of New South Wales, Sydney, NSW, Australia, [4]Australian Antarctic Program Partnership, Institute for Marine and Antarctic Studies, University of Tasmania, Hobart, TAS, Australia, [5]School of Geography, Earth and Atmospheric Sciences, University of Melbourne, Parkville, VIC, Australia, [6]Australian Research Council Centre of Excellence for the Weather of the 21st Century, University of Melbourne, Parkville, VIC, Australia

Abstract The future response of the Antarctic Slope Current (ASC) to projected transient changes in winds, radiative forcing, and meltwater input is examined in a high-resolution ocean-sea ice model. Meltwater changes are found to dominate the almost -circumpolar strengthening of the ASC. The strength of the ASC increases non-linearly despite the linear meltwater perturbation applied, with a ∼14% increase in strength from 2000 to 2025 contrasting a ∼49% increase from 2025 to 2050. This non-linear increase is, however, not seen in the coastal currents on the continental shelf. The non-linear growth of ASC strength is attributed to meltwater accumulating on the continental shelf and poleward shifting warm waters north of the ASC, both triggered by reduced dense shelf water formation, and causing an accelerating ASC through thermal wind balance. Despite the strengthening ASC, any vulnerabilities in the current system could bring poleward shifted warmer waters onto the shelf, with implications for Antarctic ice shelf melt.

Plain Language Summary The Antarctic Slope Current (ASC) is a westward current flowing around the Antarctic continent, and acts as a barrier between warm waters further north, and the cool Antarctic ice shelves. Although the ASC acts as an important barrier to the southward transport of warm water, how the ASC responds to time-varying changes in climate is unclear. We used high-resolution ocean-sea ice models to predict how the ASC will respond to changes in wind, heating, and meltwater under climate change. The ASC is projected to strengthen, with meltwater playing the biggest role. Although meltwater increases steadily over time, its impact on the ASC is dramatic, with a ∼49% increase in strength in the final 25 years of the experiments. This dramatic increase in current strength is due to contributions both onshore and offshore of the ASC. Meltwater onshore reduces the density of coastal waters, and this lightening of coastal waters lead to less dense water being exported off the continental shelf, allowing warm, salty water offshore to shift closer to the continental slope. The growing density difference across the current with time thus accelerates the ASC dramatically, and has critical implications on heat transport toward Antarctica.

1. Introduction

The Antarctic Slope Current (ASC) is a westward flowing current around Antarctica, lying close to the coast over the continental slope (Thompson et al., 2018). The ASC has been shown to regulate the cross-slope transport of warm Circumpolar Deep Water (CDW) onto the Antarctic continental shelf. This cross-slope transport depends on the local structure of the ASC and the presence of topographic features such as canyons (e.g., Daae et al., 2017; Morrison et al., 2020; Nakayama et al., 2021; Ong et al., 2024). CDW intrusions are able to transport heat poleward to the Antarctic continental shelf, which can induce basal melt and reduce buttressing of ice shelves, increasing glacial and ice sheet flow, resulting in global sea level rise (e.g.,Gudmundsson et al., 2019; Herraiz-Borreguero et al., 2016; Mathiot & Jourdain, 2023; Lauber et al., 2023).

Significant changes to the climate system around the Antarctic margin are expected under a warming climate, which can impact the structure of the ASC. Meltwater fluxes around the Antarctic margin are expected to increase, with Golledge et al. (2019) predicting a maximum meltwater flux of 0.018 Sv under the Representative Concentration Pathway (RCP) 8.5 scenario by the end of 21st Century, as well as an Antarctic Ice Sheet

contribution to sea level rise of 14 cm. Note that the meltwater projections that motivate our experimental design (Golledge et al., 2019) are at the low end of available projections, with estimated Antarctic Ice Sheet contributions to sea level rise ranging between 11 and 79 cm by 2,100 (Intergovernmental Panel on Climate Change, 2022). These increasing meltwater fluxes from ice shelves can also reduce both the formation and the transport of Antarctic Bottom Water as the meltwater freshens the water column (Li et al., 2023), countering possible increases in sea ice production resulting from iceberg melt (Mackie et al., 2020) and resulting in a 50%–60% reduction in northward AABW transport (Tesdal et al., 2023). The easterly and southerly surface winds around the Antarctic margin are additionally expected to reduce by 23% and 7% respectively under high emission scenarios (Neme et al., 2022). As surface wind changes and meltwater fluxes can influence the structure of the ASC and warm water inflow toward the Antarctic continental shelf (Daae et al., 2017; A. L. Stewart & Thompson, 2015), understanding the effect of climate change on the ASC and warm water transport onto the shelf is of imminent importance.

Despite the importance of understanding ASC changes under climate change, past research in this area has been limited. Previous work has investigated ASC changes under meltwater perturbations comparable to RCP scenarios, but these have been limited to models with 0.5° and 0.25° horizontal resolution (Beadling et al., 2022), where a stronger ASC is represented in the higher resolution model. Model experiments at higher, eddy-resolving 0.1° resolution by Moorman et al. (2020) and Dawson et al. (2025) have been conducted, in which they imposed an abrupt step increase in meltwater forcing. These studies showed that meltwater strengthens the density gradients across the continental slope, amplifying the ASC, consistent with other climate change perturbation experiments (Dawson et al., 2025; Goddard et al., 2017; Lockwood et al., 2021) and the higher resolution, 0.25°, model of Beadling et al. (2022). Dawson et al. (2025)'s study also shows that the effect of wind and thermal climate change forcings on ASC strength was much smaller than the impact of meltwater on the ASC. While Dawson et al. (2025) and Moorman et al. (2020)'s experiments give us an insight into the immediate impacts of meltwater and other climate forcings on the ASC, it is important to use a time-varying meltwater input because even under an idealized step change to projected atmospheric conditions, predictions have shown that ice shelf melt rates would still take several decades to adjust (Mathiot & Jourdain, 2023). Li et al. (2023) is the only study that used a long-term, time-varying meltwater perturbation, also finding that the ASC speeds up under increased meltwater forcing, but they did not study the ASC's transient response over the duration of the experiment. Considering the different response times that various oceanic processes have in the abrupt step change meltwater forcing experiments by Moorman et al. (2020), exploring how a more realistic time-dependent meltwater perturbation influences ASC changes is an important open area of research, which we aim to address in this study.

2. Model and Methods

This study analyses climate change experiments run using the global ocean–sea ice model, Australian Community Climate and Earth System Simulator (ACCESS-OM2-01), details of which are outlined by Kiss et al. (2020). ACCESS-OM2-01 has a lateral resolution of 0.1° and captures a realistic representation of the dynamics around the Antarctic continental margin (e.g., Dawson et al., 2023; Li et al., 2023; Schmidt et al., 2023). Huneke et al. (2022) additionally analyzed the variability of the ASC in the ACCESS-OM2-01 model, showing that zonal transports around the Antarctic continent are comparable to in-situ observations (Peña-Molino et al., 2016).

Three experiments are evaluated in this study: (a) a control experiment, (b) a wind, radiation, and thermal perturbation experiment (Wind + Thermal), and (c) a third experiment that is identical to the Wind + Thermal experiment, only with an additional future meltwater perturbation incorporated (Wind + Thermal + Meltwater). The two perturbation experiments were designed to mimic future climate scenarios, while allowing us to isolate the impact of Antarctic and Greenland Ice Sheet mass loss through meltwater anomalies.

The control experiment uses a repeat-year atmospheric forcing of the JRA55-do v1.3 product (Tsujino et al., 2018), using the forcing from 1 May 1990 to 30 April 1991, a period that is characterized by neutral conditions of the dominant climate variability modes (K. D. Stewart et al., 2020). The model was first spun up for 200 years before the perturbations were introduced. Our analyses use model years 210–260 of both the control and the perturbation experiments, a 50-year period 10 years after wind and thermal perturbations were first applied, the same experiments and period as those run and analyzed by Li et al. (2023). The wind and thermal perturbations are applied globally and are derived using near-surface anomaly fields from the JRA55-do v1.3 product (for the historical period from 1991 to 2019) and Coupled Model Intercomparison Project six projections under the high-
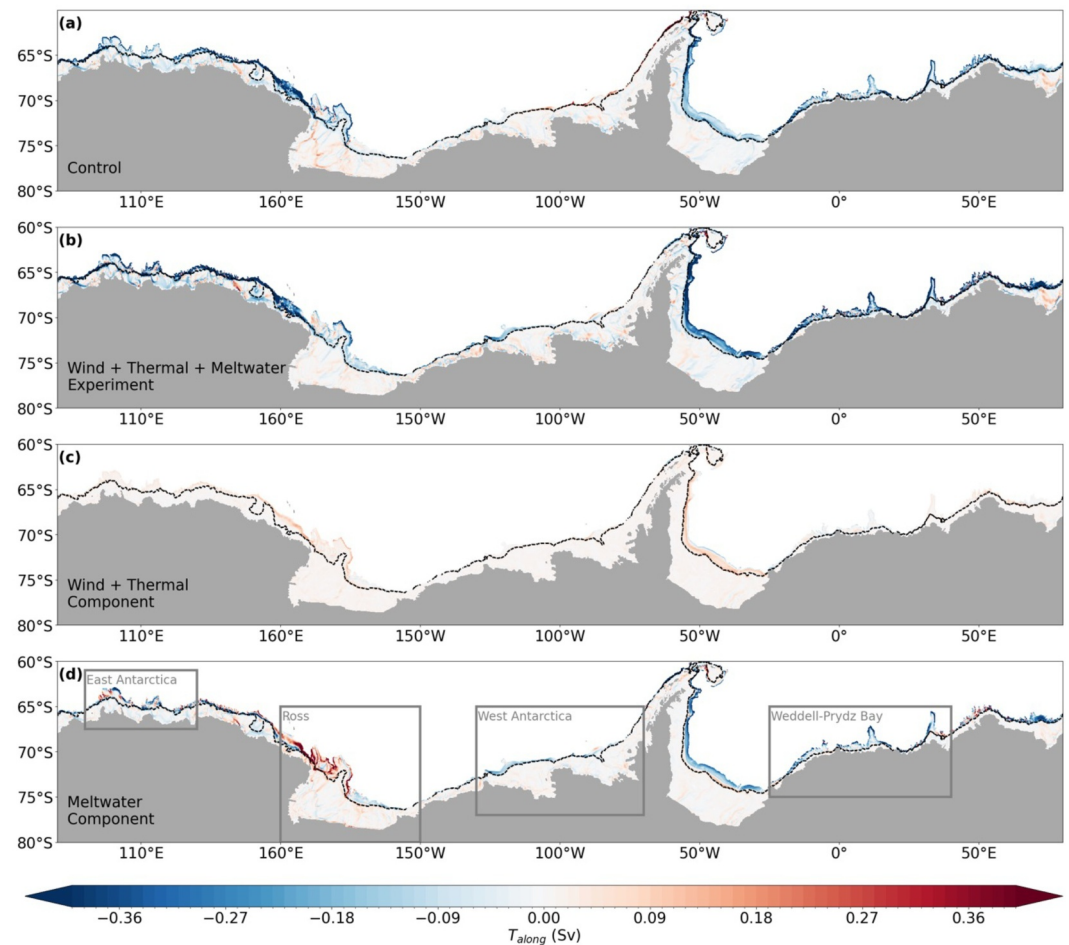
Figure 1. Along-slope depth-averaged transport averaged over 2040–2050 for the (a) Control, (b) experiment with all forcings (Wind + Thermal + Meltwater run) (c) Wind + Thermal component (Wind + Thermal run relative to the control) and the (d) Estimated meltwater component, that is, (Wind + Thermal + Meltwater run)−(Wind + Thermal run). The dotted line primarily follows the 600 m isobath, which we define to separate the Antarctic Slope Current and Antarctic Coastal Current. The boxes in panel (d) highlight the selected regions featured in Figure S1 and Figure S4 in Supporting Information S1.

anthropogenic-emissions scenario Shared Socioeconomic Pathway 5–8.5 (SSP5-8.5) (for the 2020–2050 period) (Eyring et al., 2016; O'Neill et al., 2016). The meltwater forcing is a time-varying perturbation applied at the surface directly at the coast around Greenland and Antarctica, with Greenland meltwater added uniformly around the coastline, whereas meltwater is added around Antarctica along a band of coast stretching from the Weddell Sea westward to the Ross Sea (Extended Data Figure 3d, Li et al., 2023), capturing the regions projected to exhibit a strong increase in ice sheet melt this century (Golledge et al., 2019). The total meltwater forcing around Antarctica is increased linearly from 0 to 0.08 Sv (about 2,523 Gt yr^{-1}) applied from 2001 to 2050 at a rate of 0.16 Sv per century, an approximation of Golledge et al. (2019)'s projected, gradually increasing runoff rates post 2000 under RCP8.5. This transient increase distinguishes these experiments from those by Moorman et al. (2020) and Dawson et al. (2025), who applied a step-change in meltwater forcing. Hence the gradual, although linear, increase in meltwater forcing in this study serves as a closer approximation to simulated future freshwater fluxes from the Antarctic Ice Sheet (Coulon et al., 2024).

3. Spatial Response of the ASC

We first assess the spatial changes in the ASC and Antarctic Coastal Current (ACoC) strength in each of the experiments; these are summarized in Figure 1 with plots of the along-slope transport averaged between 2040 and 2050. For these circumpolar fields and all other circumpolar quantities analyzed in this study, we exclude regions

with a water column deeper than 2500 m and select only regions adjacent to the continental shelf. Figures 1c and 1d show the change in along-slope velocity due to the different perturbations. Negative along-slope transport anomalies indicate a strengthened westward current.

The estimated meltwater component (i.e., Wind + Thermal + Meltwater run − Wind + Thermal run) in panel (d) shows that meltwater makes the greatest contribution to the ASC changes, in agreement with Beadling et al. (2022) and Dawson et al. (2025). The meltwater forcing also has the strongest impact on the slope (instead of over the continental shelf), as seen in the regional plots presented in Figure S1 in Supporting Information S1. The dotted boundary between the ASC and ACoC in Figure 1 primarily follows the 600 m isobath, where we have additionally removed regions corresponding to shelf canyons. The initial choice of the 600 m isobath, prior to removing canyon effects, is informed by the Hovmöller plot of zonal velocity in Figure S2 in Supporting Information S1. The different meltwater effects on the continental shelf and slope motivate us to distinguish these slope and shelf regions in the following analysis, focusing on temporal changes under the various climate forcings.

4. Transient Response of the ASC

### 4.1. Non-Linear ASC Response Under Meltwater Forcing

In order to assess the impact of the respective transient climate forcings, Figures 2a and 2b shows the circumpolar average of along-slope depth-averaged transport around the Antarctic continent over time, with a 12-month rolling mean applied. The transport is separated into the 'shelf' (panel a) and 'slope' (panel b) regions, following the dotted boundary shown in Figure 1. Transports in each of the 'shelf' and 'slope' regions are computed by selecting, at each longitude grid, the maximum cumulative along-slope westward transport for the chosen isobath range, then taking a circumpolar average. We find that the meltwater perturbation experiment (blue) has by far the largest influence on the along-slope velocity, with ∼71% increase throughout the duration of the experiment on the slope (panel b), but a comparatively small ∼36% increase in the shelf (ACoC) current (panel a) (Note: all percentages are reported to 2 significant figures.) The wind and thermal experiments in red exhibit a much smaller change compared to the experiments with meltwater, decreasing instead by ∼2.8% on the slope and increasing by ∼6.2% on the shelf. Despite the meltwater flux increasing linearly in time in the meltwater perturbation experiment, the strengthening slope current in the meltwater perturbation experiment shows a dramatically non-linear increase, with a ∼14% increase in the first half of the experiment but a ∼49% increase in the second half. However, the shelf currents in the meltwater perturbation experiment do not exhibit the same dramatically non-linear behavior. Furthermore, a decomposition of kinetic energy on the slope and shelf regions of the meltwater run show that the mean, rather than the eddying component of the flow, contributes to the non-linear increase in slope current transport (Text S1 and Figure S3 in Supporting Information S1), indicating that there are fundamentally different dynamics dominating the mean flow changes over the slope and shelf.

A discussion of regional variation in ASC and ACoC changes over time is included in Text S2 and Figure S4 in Supporting Information S1, but in all regions, meltwater perturbations dominate the ASC and ACoC changes under climate forcings. Considering that the non-linear increase in ASC transport is dominant enough to influence the circumpolar average, and that the meltwater component of the Wind + Thermal + Meltwater experiment drives this accelerating transport, this motivates investigating the Wind + Thermal + Meltwater experiment further to understand the role of changing hydrographic properties in driving this ASC transport increase.

### 4.2. Thermal and Saline Properties in ACoC and ASC

To investigate the changing hydrographic properties across the ASC and ACoC, we next consider the circumpolar-averaged temperature and salinity at both the onshore and offshore edge of each current. The contours following the southern continental shelf edge and the 2500 m-isobath of Figure 1 are the onshore edge of the ACoC and the offshore edge of the ASC respectively, and the 600 m-isobath separating the ASC and ACoC (dotted line in Figure 1) is taken to be the ACoC offshore and ASC onshore edge. We average over grid cells within 30-km laterally of each contour to calculate the circumpolar average. The volume-averaged temperature and salinity at the onshore ACoC edge (brown), boundary between the ACoC and ASC (navy) and the offshore ASC edge (orange) are shown in Figures 2c–2f, the difference denoted by the shading between the two lines.
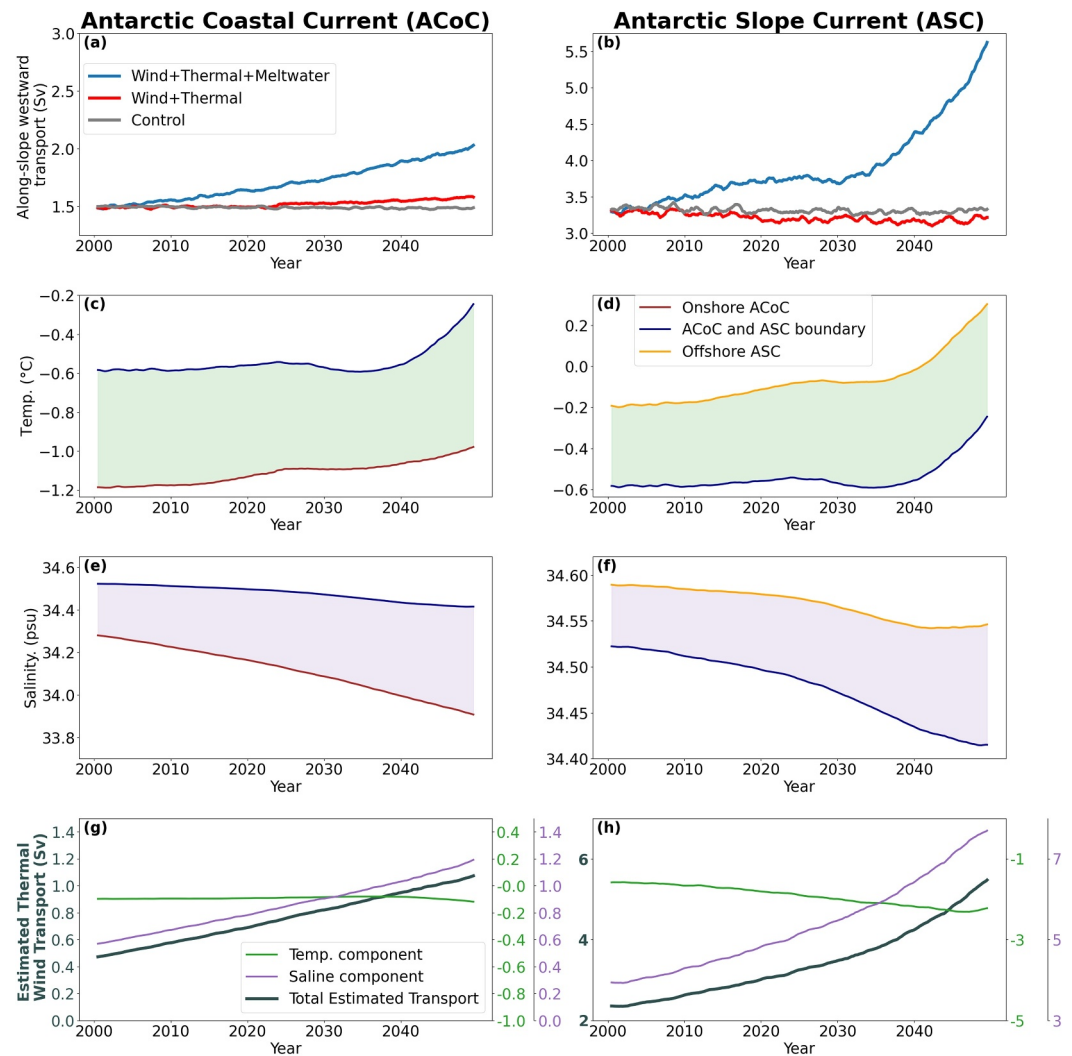
Figure 2. Circumpolar averaged along-slope westward transport from 2000 to 2050 for the Control (gray), Wind + Thermal (red) and Wind + Thermal + Meltwater (blue) experiments, on the continental shelf (a), and on the continental slope (b), analogous to the Antarctic Coastal Current (ACoC) and Antarctic Slope Current (ASC) respectively, where in this figure positive transport values are westward. The panels that follow show the Wind + Thermal + Meltwater experiment: Volume-averaged temperature within 30-km laterally of the northern and southern edges of the (c) ACoC and (d) ASC, showing the quantities for the onshore edge of the ACoC (brown), boundary between ACoC and ASC (navy), and the offshore edge of the ASC (orange). The green shading represents the temperature difference that contributes to the thermal wind balance. Volume-averaged salinity within 30-km laterally of the northern and southern edges of the (e) ACoC and (f) ASC, with the same line colors as in (c)–(d). The purple shading represents the salinity difference that contributes to the thermal wind balance. Estimated westward transport due to the thermal wind balance (gray) in the (g) ACoC and (h) ASC, based on temperature and salinity changes. The temperature (green) and saline (purple) components of the estimated transport are shown on the same plot on a different y-scale (shown on the right in each panel). A 12-month rolling mean is applied to all quantities plotted.

The resulting analysis reveals that warming occurs in all the regions analyzed of both the ACoC and ASC (Figures 2c and 2d). Moorman et al. (2023) previously showed a temporary warming followed by a long-term cooling over the shelf, and a long-term warming on the slope under an abrupt meltwater perturbation. Therefore, the increasing meltwater perturbation in this study's experiments are consistent with the initial transient shelf warming and the long-term warming on the slope. For salinity, the ASC experiences a faster increase in salinity difference across the current compared to the ACoC (Figures 2e and 2f, width of purple shading increases with time). Both currents experience more rapid freshening onshore, as the meltwater forcing increases over time. However, the offshore region of the ASC initially freshens, but its average salinity then levels off in time and
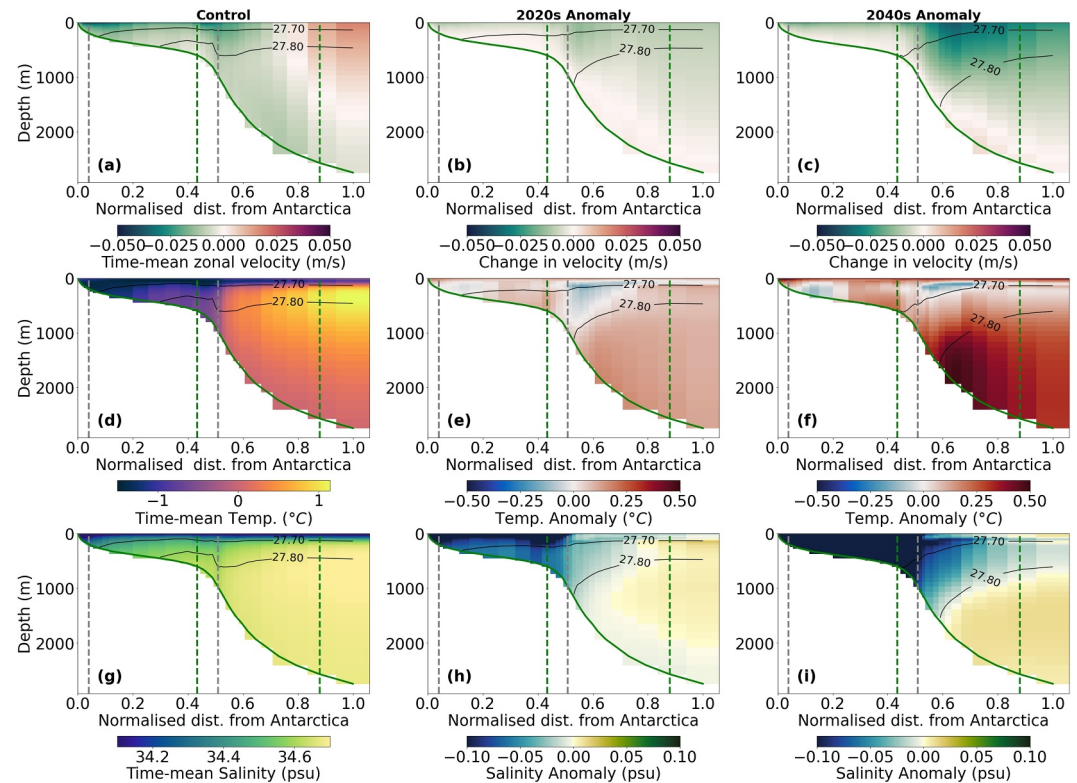
Figure 3. Cross sections of circumpolar averaged (a)–(c) zonal velocity (d)–(f) temperature, and (g)–(i) salinity around Antarctica, for (a,d,g) the control run (b,e,h) 2020s decadal anomaly of the Wind + Thermal + Meltwater experiment from the control and (c, f) 2040s decadal anomaly of the Wind + Thermal + Meltwater experiment from the control. The green dashed lines intersect with the 600 and 2500 m isobath, delineating the Antarctic Slope Current (ASC) and Antarctic Coastal Current (ACoC) regions. The gray dashed lines intersect with the 200 and 1000 m isobath, which we have defined to be the core of the ACoC and ASC respectively. Isopycnals are shown in black contours and are labeled by their anomaly from 1000 kg/m^3.

rebounds slightly after 2040, amplifying the non-linear increase in salinity gradient. This salinification is driven by offshore CDW encroaching poleward on the continental slope, as documented in Li et al. (2023), due to the heaving/descent of isopycnals spreading CDW polewards and downwards, allowing for a leveling off in time of salinity offshore of the ASC. These circumpolar-averaged quantities indicate that it is possible for the temperature and salinity differences to drive a non-linear increase in ASC strength.

4.3. Thermal Wind Balance

Using the onshore/offshore temperature and salinity values for the ASC and ACoC, we can use thermal wind balance to estimate a theoretical westward geostrophic transport, to determine if the changing hydrographic properties directly control the non-linear increase in ASC strength, as inspired by Sohail et al. (2025) and Sohail and Zika (2024). Assuming geostrophic flow, a flat bottom, and a uniform flow across the current domain, we use the thermal wind balance $f \partial u / \partial z \sim (g/\rho) \partial \rho / \partial y$ to estimate the geostrophic zonal velocity $u \sim (gH\Delta\rho)/\rho_0 fW$, where ρ_0 is a reference density and $\Delta\rho$ is the meridional change in density across the domain, $g = 9.81 \text{m/s}^2$ is the gravitational acceleration, $f = -1.3 \times 10^{-4} \text{ s}^{-1}$ is the Coriolis parameter, H is the depth of flow and W is the width of the current. The evolution of zonal transport T with time is therefore:

$$\mathrm{T} \sim \frac{gH^2}{f} \overbrace{\left(\underbrace{-\alpha\Delta\Theta}_{\text{thermal component}} + \underbrace{\beta\Delta S}_{\text{saline component}}\right)}^{=\Delta\rho/\rho_0},\tag{1}$$

where H is the depth of flow, with $H_{ASC} = 1000$ m and $H_{ACoC} = 200$ m, $\alpha = 5.37 \times 10^{-5\circ}\,\mathrm{K}^{-1}$ is the thermal expansion coefficient, $\beta = 7.78 \times 10^{-4}\,\mathrm{psu}^{-1}$ is the haline contraction coefficient, where a volume-averaged α and β was computed over the Antarctic slope and shelf in the Wind + Thermal + Meltwater experiment. $\Delta\Theta$ and ΔS are the differences in a volume averaged temperature and salinity onshore and offshore of the current in question over time, using the quantities from Figures 2c–2f.

The estimated westward ACoC and ASC transport due to thermal wind balance is plotted in dark blue in Figures 2g and 2h respectively. The shear transport of the ACoC due to thermal wind balance increases linearly over time, but that of the ASC exhibits a non-linear increase. The thermal and saline components of the thermal wind transport in Equation 1 are shown in green and purple respectively, showing that the saline component contributes to the non-linear increase in ASC strength seen after 2040. Although the exact transport values vary depending on the parameters chosen and the definitions of the ASC/ACoC onshore and offshore regions, within a 25% deviation of H_{ASC}, α and β, the non-linear trend in the saline component of the ASC remains robust. As the along-slope transport of the ASC due to the mean-flow of Figure 2a has similar behavior under meltwater perturbations as the transport predicted by the saline-component of the thermal wind balance (and no such relation is seen for the thermal component), the evolving salinity gradient across the ASC is likely the governing driver of this increased acceleration of the ASC with time.

We evaluate the role of poleward shifting CDW in the acceleration of the ASC in the second half of the meltwater experiment by looking at circumpolar averages of zonal velocity, temperature, and salinity cross-sections around the Antarctic continent (Figure 3). The cross-sections are binned by water column depth at each grid cell, and scaled in the latitudinal direction by the area of grid cells at each depth level. To corroborate the non-linear increase in ASC transport seen in Figures 2b and 2h, we compare the middle (2020s) and final (2040s) decade of the experiment to the control run. Between the control run and the later years of the meltwater experiment, the zonal velocity on the slope increases dramatically, especially when comparing the anomaly from the first half (b) of the experiment to the second half (c). The strengthened ASC coincides with greater warming (Figures 3e and 3f) and salinification (Figures 3g and 3h) in the lower continental slope in the second half of the experiment than the first, due to the poleward shifting CDW and the shutdown of dense shelf water (DSW) formation. The timing of the shutdown of DSW formation matches the reduction in the Antarctic Bottom Water transport in Figure 3a of Li et al. (2023), where in these same experiments as in this study, the Antarctic Bottom Water transport decreases from 2030 onward. As Li et al. (2023) outlined, the reduction in DSW formation, and the contraction of the DSW water mass brings CDW closer to the continental shelf, resulting in a strong warming signal and slight salinification at depth in the final decade of the experiment. The effects of salinification at depth due to CDW are compounded by the surface freshening due to meltwater, where the reduced DSW export limits offshore flow, isolating the shelf from the offshore waters, and allows meltwater to accumulate on the shelf (Figures 3h and 3i), further strengthening the salinity gradient across the continental slope, accelerating the ASC through the saline component of the thermal wind balance. The hydrography in these averaged cross-sections is therefore consistent with the increased acceleration of the ASC toward the middle of the 21st Century (Figure 3c). We therefore propose that the shutdown of DSW formation from 2030 onwards, the accumulation of freshwater on the continental shelf and the poleward shifting of CDW drives a non-linear acceleration of the ASC, even under a linear increase in meltwater forcing.

5. Conclusions

This study finds that the ASC and ACoC are most influenced by meltwater forcing in climate change experiments, consistent with previous studies (Beadling et al., 2022; Dawson et al., 2025). We find that under a transient, linearly increasing meltwater perturbation around the Antarctic margin, mimicking the enhanced melting under an RCP8.5 scenario, the ASC accelerates more rapidly toward the middle of the 21st Century (see schematic in Figure 4). Initially, meltwater input around the Antarctic continent gradually freshens the continental shelf and slope, increasing the salinity gradient across the ASC and ACoC, as the onshore regions are freshened more
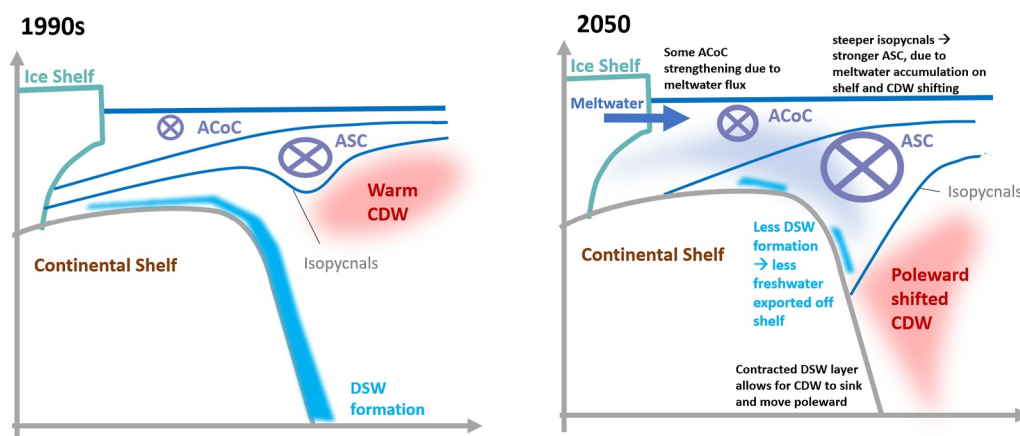
Figure 4. Schematic showing key processes before and after the addition of transient meltwater in the 1990s and 2050 respectively. Upon the transient addition of meltwater, the surface waters around Antarctica freshen, steepening isopycnals and driving the speeding up of the Antarctic Coastal Current. As the surface freshening on the continental shelf inhibits the formation and export of dense shelf water, warm Circumpolar Deep Water sinks and shifts poleward. This warm and salty water strengthens the salinity gradient over the continental slope and causes the non-linear acceleration of the Antarctic Slope Current.

rapidly than the offshore regions. The freshening of the continental shelf reduces the formation of DSW, reducing the export of DSW from 2030 onward, as quantified by Li et al. (2023). Thus, a positive feedback is set up, where freshening of the shelf not only reduces DSW formation and export, but the reduced DSW export also removes a pathway for water to exit the continental shelf. This isolates the continental shelf from the offshore region, allowing meltwater to accumulate on the shelf and further freshen the onshore region, steepening the density gradient across the ASC. From 2040 onwards, the poleward shifting of warm CDW continues to steepen the salinity gradient on the continental slope, further strengthening the ASC through thermal wind balance. As the ACoC does not experience the poleward shifted CDW, its strengthening is limited compared to the ASC. These results indicate that the ASC would more strongly isolate the continental shelf from the greater Southern Ocean, as on average, the ASC gets stronger and DSW formation is reduced around the continent. Regional differences mean that the exact processes in the schematic of Figure 4 would not be featured everywhere around Antarctica. However, the key governing processes: that reduced DSW formation leads to a fresher continental shelf and saltier lower continental slope, leading to a non-linear acceleration of the ASC, is still consistent with regional trends (Figure S4 in Supporting Information S1). Dense shelf water formation regions of the Antarctic marginal ocean therefore undergo a regime change from a DSW forming "dense regime" to a surface intensified ASC in a "fresh shelf regime", as defined by Thompson et al. (2018) and Huneke et al. (2022), with possible implications for warm water access to the continental shelf and feedbacks on ice shelf melt.

There are several limitations to this study and addressing them would be worthwhile future work. Using a coupled climate model instead of an ocean only model would capture feedback between the ocean and atmosphere excluded from this current study. However, Li et al. (2023) compared this study's experiment with meltwater to a similar coupled experiment (Purich & England, 2023), finding that meltwater has a limited impact on atmospheric circulation in the mid-to-high latitudes. Thus, a coupled model study would primarily investigate second-order impacts of meltwater on the ASC system. Although the 0.1° horizontal resolution used in the simulations is eddy-permitting, it is not fully eddy-resolving at high latitudes nor does our model include tidal effects, both of which play an important role in ASC dynamics and the poleward intrusions of CDW (e.g., A. L. Stewart et al., 2018; Si et al., 2022). In particular, Si et al. (2023) showed in an eddy- and tide-resolving model that the freshening of the Antarctic shelf and steepening of the slope front can induce baroclinic instabilities, allowing for warm CDW to be transported poleward. Furthermore, the ASC regime change under meltwater input means that additional effects that may be present in the fresh shelf regime could now take effect in previously dense shelf regime regions, for example, the intrinsic variability of CDW intrusions and the ASC (Ong et al., 2024). Considering that CDW shifting poleward is driving the further acceleration of the ASC, that this study is not fully eddy-resolving, and that eddy and tidal processes are not represented in this experiment, the impacts of this non-linearly accelerating ASC on cross-slope heat transport still remain unclear. Establishing whether the accelerating

ASC obstructs or enables the access of CDW to the shelf under this changing ASC regime is therefore an important area of future work.

The projected increasing acceleration of the ASC has implications on future changes around the Antarctic margin. Understanding the interplay between the sinking and poleward shifting of CDW and the speed-up of the ASC remains an open area of research. While the strengthened ASC can act as a barrier to keep CDW off the continental shelf, any vulnerabilities in this frontal system could expose the Antarctic shelf to greater amounts of warm CDW intrusion. Therefore, investigating transient responses around the Antarctic margin and understanding the stability of the ASC is of particular importance in a warming world.

Data Availability Statement

The ACCESS-OM2-01 model simulation output is available on the Australian National Computing Infrastructure in the Consortium for Ocean–Sea Ice Modelling in Australia (COSIMA, LP200100406) Model Output Collection at the Australian National University (2020). The scripts used for analysing model output and generating figures are available at Ong (2025).

References

Australian National University. (2020). *COSIMA Model Output Collection (Version 1)*. NCI Australia. https://doi.org/10.4225/41/5A2DC8543105A

Beadling, R. L., Krasting, J. P., Griffies, S. M., Hurlin, W. J., Bronselaer, B., Russell, J. L., et al. (2022). Importance of the Antarctic slope current in the Southern Ocean response to ice sheet melt and wind stress change. *Journal of Geophysical Research: Oceans*, *127*(5). https://doi.org/10.1029/2021JC017608

Coulon, V., De Rydt, J., Gregov, T., Qin, Q., & Pattyn, F. (2024). Future freshwater fluxes from the Antarctic ice sheet. *Geophysical Research Letters*, *51*(23), 1–12. https://doi.org/10.1029/2024GL111250

Daae, K., Hattermann, T., Darelius, E., & Fer, I. (2017). On the effect of topography and wind on warm water inflow—An idealized study of the southern Weddell Sea continental shelf system. *Journal of Geophysical Research: Oceans*, *122*(3), 2622–2641. https://doi.org/10.1002/2016JC012541

Dawson, H. R. S., England, M. H., Morrison, A. K., & Dias, F. B. (2025). End-of-21st century changes on the Antarctic continental shelf under mid- and high-range emissions scenarios. https://doi.org/10.22541/au.174180417.77812513/v1

Dawson, H. R. S., Morrison, A. K., England, M. H., & Tamsitt, V. (2023). Pathways and timescales of connectivity around the Antarctic continental shelf. *Journal of Geophysical Research: Oceans*, *128*(2). https://doi.org/10.1029/2022JC018962

Eyring, V., Bony, S., Meehl, G. A., Senior, C. A., Stevens, B., Stouffer, R. J., & Taylor, K. E. (2016). Overview of the coupled model Inter-comparison project phase 6 (CMIP6) experimental design and organization. *Geoscientific Model Development*, *9*(5), 1937–1958. https://doi.org/10.5194/gmd-9-1937-2016

Goddard, P. B., Dufour, C. O., Yin, J., Griffies, S. M., & Winton, M. (2017). CO2-Induced ocean warming of the Antarctic continental shelf in an eddying global climate model. *Journal of Geophysical Research: Oceans*, *122*(10), 8079–8101. https://doi.org/10.1002/2017JC012849

Golledge, N. R., Keller, E. D., Gomez, N., Naughten, K. A., Bernales, J., Trusel, L. D., & Edwards, T. L. (2019). Global environmental consequences of twenty-first-century ice-sheet melt. *Nature*, *566*(7742), 65–72. https://doi.org/10.1038/s41586-019-0889-9

Gudmundsson, G. H., Paolo, F. S., Adusumilli, S., & Fricker, H. A. (2019). Instantaneous Antarctic ice sheet mass loss driven by thinning ice shelves. *Geophysical Research Letters*, *46*(23), 13903–13909. https://doi.org/10.1029/2019GL085027

Herraiz-Borreguero, L., Church, J. A., Allison, I., Peña-Molino, B., Coleman, R., Tomczak, M., & Craven, M. (2016). Basal melt, seasonal water mass transformation, ocean current variability, and deep convection processes along the Amery Ice Shelf calving front, East Antarctica. *Journal of Geophysical Research: Oceans*, *121*(7), 4946–4965. https://doi.org/10.1002/2016JC011858

Huneke, W. G. C., Morrison, A. K., & Hogg, A. M. (2022). Spatial and subannual variability of the Antarctic slope current in an eddying ocean–sea ice model. *Journal of Physical Oceanography*, *52*(3), 347–361. https://doi.org/10.1175/JPO-D-21-0143.1

Intergovernmental Panel on Climate Change. (2022). The ocean and cryosphere in a changing climate. https://doi.org/10.1017/9781009157964

Kiss, A. E., McC Hogg, A., Hannah, N., Boeira Dias, F., B Brassington, G., Chamberlain, M. A., et al. (2020). ACCESS-OM2 v1.0: A global ocean-sea ice model at three resolutions. *Geoscientific Model Development*, *13*(2), 401–442. https://doi.org/10.5194/gmd-13-401-2020

Lauber, J., Hattermann, T., de Steur, L., Darelius, E., Auger, M., Nøst, O. A., & Moholdt, G. (2023). Warming beneath an East Antarctic ice shelf due to increased subpolar westerlies and reduced sea ice. *Nature Geoscience*, *16*(10), 877–885. https://doi.org/10.1038/s41561-023-01273-5

Li, Q., England, M. H., Hogg, A. M., Rintoul, S. R., & Morrison, A. K. (2023). Abyssal ocean overturning slowdown and warming driven by Antarctic meltwater. *Nature*, *615*(7954), 841–847. Retrieved from https://www.nature.com/articles/s41586-023-05762-wdoi:10.1038/s41586-023-05762-w

Lockwood, J. W., Dufour, C. O., Griffies, S. M., & Winton, M. (2021). On the role of the Antarctic slope front on the occurrence of the Weddell Sea Polynya under climate change. *Journal of Climate*, *34*(7), 2529–2548. Retrieved from https://journals.ametsoc.org/view/journals/clim/34/7/JCLI-D-20-0069.1.xmldoi:10.1175/JCLI-D-20-0069.1

Mackie, S., Smith, I. J., Ridley, J. K., Stevens, D. P., & Langhorne, P. J. (2020). Climate response to increasing Antarctic iceberg and ice shelf melt. *Journal of Climate*, *33*(20), 8917–8938. Retrieved from https://journals.ametsoc.org/doi/10.1175/JCLI-D-19-0881.1doi:10.1175/JCLI-D-19-0881.1

Mathiot, P., & Jourdain, N. C. (2023). Southern Ocean warming and Antarctic ice shelf melting in conditions plausible by late 23rd century in a high-end scenario. *Ocean Science*, *19*(6), 1595–1615. https://doi.org/10.5194/os-19-1595-2023

Moorman, R., Morrison, A. K., & Hogg, A. M. C. (2020). Thermal responses to Antarctic ice shelf melt in an Eddy-Rich global ocean-sea ice model. *Journal of Climate*, *33*(15), 6599–6620. https://doi.org/10.1175/JCLI-D-19-0846.1

Moorman, R., Thompson, A. F., & Wilson, E. A. (2023). Coastal polynyas enable transitions between high and low west Antarctic ice shelf melt rates. *Geophysical Research Letters*, *50*(16). https://doi.org/10.1029/2023GL104724

Morrison, A. K., Hogg, A. M., England, M. H., & Spence, P. (2020). Warm Circumpolar Deep Water transport toward Antarctica driven by local dense water export in canyons. *Science Advances*, *6*(18). https://doi.org/10.1126/sciadv.aav2516

Nakayama, Y., Greene, C. A., Paolo, F. S., Mensah, V., Zhang, H., Kashiwase, H., et al. (2021). Antarctic slope current modulates ocean heat intrusions towards Totten glacier. *Geophysical Research Letters*, *48*(17). https://doi.org/10.1029/2021GL094149

Neme, J., England, M. H., & McC. Hogg, A. (2022). Projected changes of surface winds over the Antarctic continental margin. *Geophysical Research Letters*, *49*(16). https://doi.org/10.1029/2022GL098820

O'Neill, B. C., Tebaldi, C., Van Vuuren, D. P., Eyring, V., Friedlingstein, P., Hurtt, G., et al. (2016). The scenario model Intercomparison project (ScenarioMIP) for CMIP6. *Geoscientific Model Development*, *9*(9), 3461–3482. https://doi.org/10.5194/gmd-9-3461-2016

Ong, E. Q. Y. (2025). ongqingyee/MW-perturb-ASC: Accepted version with corrected transports [Dataset]. *Zenodo*. https://doi.org/10.5281/zenodo.15293170

Ong, E. Q. Y., Doddridge, E., Constantinou, N. C., Hogg, A. M., & England, M. H. (2024). Intrinsically episodic Antarctic shelf intrusions of circumpolar deep water via canyons. *Journal of Physical Oceanography*, *54*(5), 1195–1210. https://doi.org/10.1175/JPO-D-23-0067.1

Peña-Molino, B., McCartney, M. S., & Rintoul, S. R. (2016). Direct observations of the Antarctic slope current transport at 113°E. *Journal of Geophysical Research: Oceans*, *121*(10), 7390–7407. https://doi.org/10.1002/2015JC011594

Purich, A., & England, M. H. (2023). Projected impacts of Antarctic meltwater anomalies over the twenty-first century. *Journal of Climate*, *36*(8), 2703–2719. https://doi.org/10.1175/JCLI-D-22-0457.1

Schmidt, C., Morrison, A. K., & England, M. H. (2023). Wind– and sea-ice–driven interannual variability of Antarctic bottom water formation. *Journal of Geophysical Research: Oceans*, *128*(6). https://doi.org/10.1029/2023JC019774

Si, Y., Stewart, A. L., & Eisenman, I. (2022). Coupled ocean/sea ice dynamics of the Antarctic Slope Current driven by topographic eddy suppression and sea ice momentum redistribution. *Journal of Physical Oceanography*, *52*(7), 1563–1589. https://doi.org/10.1175/JPO-D-21-0142.1

Si, Y., Stewart, A. L., & Eisenman, I. (2023). Heat transport across the Antarctic Slope front controlled by cross-slope salinity gradients. *Science Advances*, *9*(18). https://doi.org/10.1126/sciadv.add7049

Sohail, T., Gayen, B., & Klocker, A. (2025). Decline of Antarctic Circumpolar Current due to polar ocean freshening. *Environmental Research Letters*, *20*(3), 034046. https://doi.org/10.1088/1748-9326/adb31c

Sohail, T., & Zika, J. D. (2024). Unsupervised classification identifies warm, fresh, and dense regimes of the Antarctic margins. *Journal of Physical Oceanography*, *54*(6), 1229–1242. https://doi.org/10.1175/JPO-D-23-0153.1

Stewart, A. L., Klocker, A., & Menemenlis, D. (2018). Circum-antarctic shoreward heat transport derived from an eddy- and tide-resolving simulation. *Geophysical Research Letters*, *45*(2), 834–845. https://doi.org/10.1002/2017GL075677

Stewart, A. L., & Thompson, A. F. (2015). Eddy-mediated transport of warm circumpolar deep water across the Antarctic shelf break. *Geophysical Research Letters*, *42*(2), 432–440. https://doi.org/10.1002/2014GL062281

Stewart, K. D., Kim, W. M., Urakawa, S., Hogg, A. M. C., Yeager, S., Tsujino, H., et al. (2020). 3). JRA55-do-based repeat year forcing datasets for driving ocean–sea-ice models. *Ocean Modelling*, *147*, 101557. https://doi.org/10.1016/j.ocemod.2019.101557

Tesdal, J. E., MacGilchrist, G. A., Beadling, R. L., Griffies, S. M., Krasting, J. P., & Durack, P. J. (2023). Revisiting interior water mass responses to surface forcing changes and the subsequent effects on overturning in the Southern Ocean. *Journal of Geophysical Research: Oceans*, *128*(3). https://doi.org/10.1029/2022JC019105

Thompson, A. F., Stewart, A. L., Spence, P., & Heywood, K. J. (2018). The Antarctic slope current in a changing climate. *Reviews of Geophysics*, *56*(4), 741–770. https://doi.org/10.1029/2018RG000624

Tsujino, H., Urakawa, S., Nakano, H., Small, R. J., Kim, W. M., Yeager, S. G., et al. (2018). JRA-55 based surface dataset for driving ocean–sea-ice models (JRA55-do). *Ocean Modelling*, *130*, 79–139. https://doi.org/10.1016/j.ocemod.2018.07.002